

# Multi-scale Geometry-aware Transformer for 3D Point Cloud Classification

Xian Wei  
TUM

xian.wei@tum.de

Muyu Wang  
Liaoning Technical University

598477187@qq.com

Shing-Ho Jonathan Lin  
University of Chinese Academy of Sciences

linchenghao21@mailsucas.ac.cn

Zhengyu Li

East China Normal University

lzy1999729@gmail.com

Jian Yang  
Information Engineering University

jian.yang@tum.de

Arafat Al-Jawari  
University of Chinese Academy of Sciences

arafatmmj@gmail.com

XUAN TANG  
East China Normal University  
2265275624@qq.com

## Abstract

Self-attention modules have demonstrated remarkable capabilities in capturing long-range relationships and improving the performance of point cloud tasks. However, point cloud objects are typically characterized by complex, disordered, and non-Euclidean spatial structures with multiple scales, and their behavior is often dynamic and unpredictable. The current self-attention modules mostly rely on dot product multiplication and dimension alignment among query-key-value features, which cannot adequately capture the multi-scale non-Euclidean structures of point cloud objects. To address these problems, this paper proposes a self-attention plug-in module with its variants, Multi-scale Geometry-aware Transformer (MGT). MGT processes point cloud data with multi-scale local and global geometric information in the following three aspects. At first, the MGT divides point cloud data into patches with multiple scales. Secondly, a local feature extractor based on sphere mapping is proposed to explore the geometry inner each patch and generate a fixed-length representation for each patch. Thirdly, the fixed-length representations are fed into a novel geodesic-based self-attention to capture the global non-Euclidean geometry between patches. Finally, all the modules are integrated into the framework of MGT with an end-to-end training scheme. Experimental results demonstrate that the MGT vastly increases the capability of capturing multi-scale geometry using the self-attention mechanism and achieves strong competitive performance

on mainstream point cloud benchmarks.

## 1. Introduction

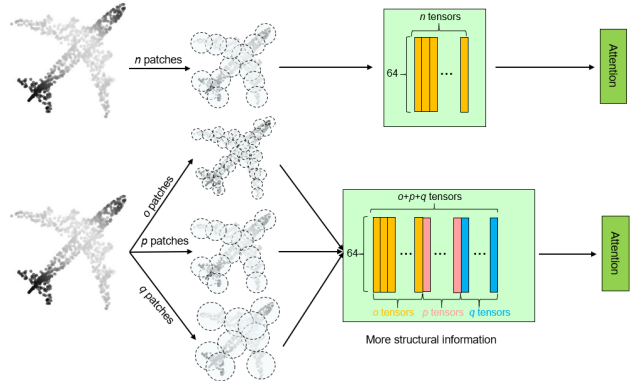


Figure 1. Comparison between traditional point cloud Transformer and MGT. MGT contains more structural information. Top: Point Cloud Transformer. Bottom: MGT.

Point cloud data is a widely used form of 3D data in fields such as autonomous driving [3, 29, 34, 7], augmented reality, and robotics [27]. However, unlike traditional images, point cloud data has complex global and local structures that are non-Euclidean in nature, making extracting features in practical applications challenging.

To address this challenge, researchers have proposed various deep learning-based 3D point cloud classification

methods, which can be categorized into voxel-based methods [20, 28], multi-view methods [13, 42], and point set methods [23, 24, 36, 35]. Voxel-based methods usually disrupt important spatial relationships in the measurement space. Multi-view methods project 3D cloud data into 2D images, resulting in the model’s inability to fully capture geometric information and spatial relationships. PointNet [23] is a pioneer in point set methods, which uses spatial encoding for each point, such as multi-layer perceptrons (MLP) and pooling layers with shared weights, to collect point set features. Despite attempts to enhance these techniques in previous work [30], they still have limited ability to capture variations in local features. Therefore, all of these algorithms are unable to fully extract the complex geometric structure of point clouds for classification.

Recently, the Transformer [32], with a self-attention mechanism at its core, has been widely applied in natural language processing (NLP), image recognition, and object detection [26, 49, 12, 6, 14]. Inspired by the tremendous success of Transformers in NLP and image domains, some researchers have attempted to introduce self-attention mechanisms into the point cloud classification field. For example, Point Cloud Transformer [47, 8] uses self-attention mechanisms to capture the relationships between points and obtain global features. However, the aforementioned self-attention modules heavily rely on dot products in the Euclidean space.

In summary, the traditional data processing methods are no longer sufficient to handle the complex non-Euclidean structure of point cloud objects. Currently, a powerful feature extractor Transformer is needed to enhance the geometry of the point cloud and improve the local feature extraction capability while utilizing the Transformer’s strong global feature acquisition ability. To this end, this paper proposes a novel Transformer, called the Multi-Scale Geometry-aware Transformer (*MGT*), to extract complex geometric structures in point clouds for classification. *MGT* divides the point cloud data into multiple patches with different numbers and sizes, thereby obtaining point cloud features from multiple scales. Figure 1 shows the comparison between traditional single-scale point cloud transformers and *MGT*. Also, this self-attention method uses geodesic distance [18] instead of dot product multiplication in the self-attention module, which is more reasonable for processing point cloud data. Figure 4 provides a simple comparison between dot product attention and geodesic attention. Additionally, this paper proposes a Shared Local Feature Extractor (SLFE) module based on a sphere mapping algorithm to extract point cloud features using a feature extraction algorithm that is more suitable for point cloud data.

The main contributions of this paper are summarized as:

- **Multi-scale Patch Division Transformer.** *MGT* divides point cloud data into multi-scale patches with

different sizes, i.e., from small size to large size of patches, and feeds them into the transformer to explore the multiple scales of structures of point clouds.

- **Geometry-aware intra-patch representation.** This paper presents an SLFE module that enhances intra-patch local features and outputs a fixed-length vector for each patch. In the SLFE module, a novel operator, called sphere mapping, is presented to capture the local geometric structure of the neighbors of a patch, i.e., the angles between points in a patch.
- **Geometry-aware inter-patch representation.** We adopt a new self-attention mechanism based on computing geodesic distances to better capture the global features between patches.

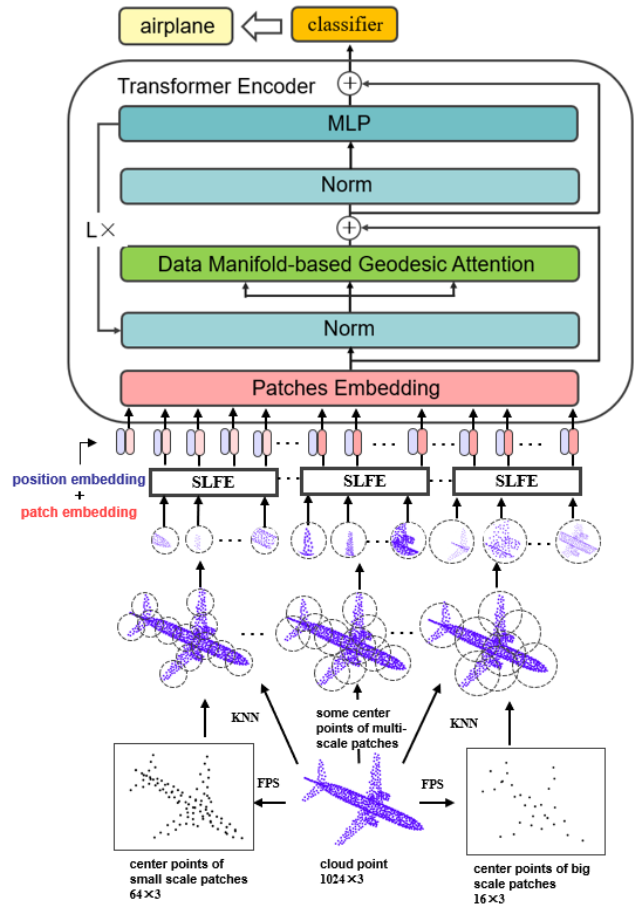


Figure 2. Model Overview. The Transformer Encoder architecture is adopted from ViT and the input data shown in Figure 1 are three-dimensional coordinates.

## 2. Related Works

### 2.1. Transformer in Visual field

Recently, relying on powerful sequential data processing and global features aggregation capabilities, Transformers have achieved great success in NLP and CV. Transformer [32], with architecture based on self-attention, consists of no recursive nor convolutional components. BERT [4] is a robust bidirectional Transformer architecture in the NLP field that handles multi-modal tasks [40]. Researchers aimed to integrate point clouds and multi-view data using the Point View Network (PVNet) [48]. In [5], a standard Transformer was applied to image patches based on pre-trained CNN models. These patches were then split into medium-sized tokens (words) for the Transformer’s input, but the method had a high bias when there was no large training set.

Self-attention networks are also used in 2D image processing due to the effectiveness of the Transformer model in NLP. [33] proposed a stack of attention and residual attention for image classification. [25] applied self-attention to local image patches, aiming to develop a local self-attention layer that works on small and large inputs in vision models. [45] developed a family of self-attention operators, and ViT divides the image into patches of equal size, using them as an input sequence for the Transformer Encoder. Experiments show that ViT performs strongly with sufficient training data.

### 2.2. Transformer for Point Cloud Classification

3D point clouds, a prevalent topic in computer vision, can be considered a special type of sequential data, making the use of Transformers a natural fit for point cloud task processing. Xie et al. [39] proposed ShapeContextNet, which hierarchically constructs patches using a context method of convolution and uses a self-attention mechanism to combine the selection and feature aggregation processes into a training operation. Point2sequence [19] starts with local areas and creates local features using LSTM-based attention modules, then uses a pooling method (referencing PointNet, Deep Sets [44]) to generate a global feature vector. Because it relies on the structure of sequences, this leads to higher computational complexity than the multi-head attention mechanism [32].

Recent studies have discovered better methods to deal with point cloud data by Transformer. Point Cloud Transformer [47, 8] of the first works to use Transformers for point cloud tasks, was recently made with a self-attention mechanism based on Edgeconv [36]. Point Cloud Transformer first increases the dimension of each point, then uses a Transformer to capture the relationships between points to obtain global features. Point-BERT [43] designs a discrete Variational AutoEncoder (dVAE) for generating point to-

kens, inspired by [4], successfully introducing BERT-style [15] pre-training to point cloud tasks. Inspired by Masked Auto Encoders (MAE) [11], Point-MAE [22] further explores pre-training methods for point cloud Transformers, implementing a pre-training pipeline for point cloud tasks with a completely standard Transformer structure. These works lay a solid foundation for future Transformer use in point cloud tasks.

In addition, some methods also use deep neural network structures and take the raw point cloud as their input. PointNet [23] is a pioneer of this type of method, which uses permutation-invariant operators (such as shared-weight MLPs and pooling layers) to aggregate features of a set of points. PointNet++ [24] further explores this idea by introducing a hierarchical spatial structure that can capture the local features of point clouds. These methods are inspiring for extracting both global and local features from point clouds.

## 3. Method

In this section, we introduce the *MGT* model, an end-to-end Transformer framework that fully explores the geometric structures of point cloud objects. At first, to examine the multiple scales of the structures of point clouds, we split the data into multi-scale patches with different sizes, i.e., from small to large patches. Then, we design a geometry-aware transformer model, which explores two-level geometric structures, i.e., the Euclidean geometry of each intra-patch and the non-Euclidean geometry of inter-patches of point clouds.

### 3.1. The MGT Framework

With divided multi-scale patches, Figure 2 depicts the pipeline of the *MGT* model, which assembles two basic modules. First, the *intra-patch representation* module for geometry-aware feature extraction of each patch. Second, the *inter-patch representation* module for learning manifold-based self-attention of multi-scale patches. The former extracts the local geometric characteristics and generates a fixed-length invariant representation vector for each patch, and the latter explores the non-Euclidean relation between multi-scale patches. The former is achieved by a developed local sharing feature extractor associated with a sphere mapping module, and a manifold-based self-attention module achieves the latter.

Before introducing the *MGT* model, we first describe the patch division of point clouds.

**Multi-scale Patch Division** In the first layer of the *MGT* model, a multi-scale patch division is performed. As shown in Figure 2, formally, given input point cloud data  $X = \{x_1, x_2, \dots, x_N\} \in R^{N \times C_{in}}$  with  $N$  points of each object,

where  $C_{in} = 3$  when only using raw position coordinates, and  $C_{in} = 6$  when adding extra normal vector [23].

For applying the multi-scale patch division, it is critical to determine the center of each patch. Using the farthest point sampling (FPS),  $S^\eta$  points are selected to treat as the center points, the set of which is denoted by  $CT^\eta$ , where  $\eta$  denotes the multiple scales of patches. Given a center point, the  $K$ -nearest neighbors algorithm (KNN) is used to select the nearest  $K^\eta$  points and form a point cloud patch  $P^\eta$  with the size of  $K^\eta \times C_{in}$ . Hence,  $CT$  denotes the set of all patches with multiple scales/sizes, from small to large.

The patch size  $K^\eta$  varies according to the different implementation settings based on used datasets. For example, in a numerical experiment, we set 4 kinds of scales/sizes for each patch, e.g., the patch size  $K^\eta = 32, 64, 128, 256$  with the kind of scales  $\eta = 1, 2, 3, 4$ , and the corresponding number of patches  $S^\eta = 64, 32, 16, 8$  with  $S = \sum_{\eta=1}^4 S^\eta$ .

Finally, for the  $\eta^{th}$  scale of point cloud patches, the patch centers and the patches can be denoted by:

$$\begin{aligned} CT^\eta &= \text{FPS}(X), CT^\eta \in R^{S^\eta \times C_{in}}, \\ P^\eta &= \text{KNN}(K^\eta, X, CT^\eta), P^\eta \in R^{S^\eta \times K^\eta \times C_{in}}. \end{aligned} \quad (1)$$

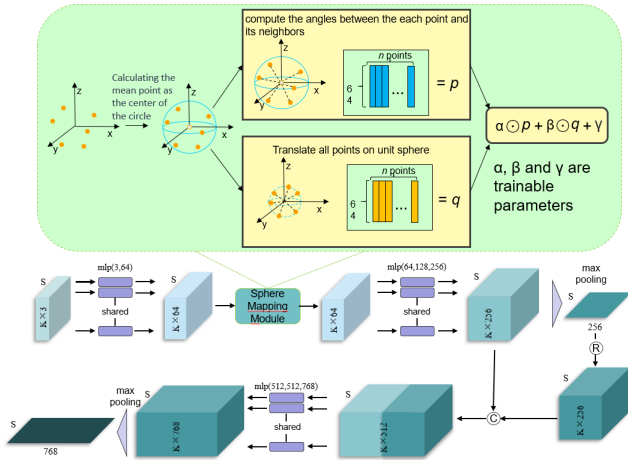


Figure 3. Overview of the proposed *SLFE* pipeline and the sphere mapping module. The input data are three-dimensional coordinates, without normal vectors.  $S^\eta, K^\eta$  are abbreviated as  $S$  and  $K$ , respectively. ‘ $\otimes$ ’ represents repeat, ‘ $\odot$ ’ represents splicing.

### 3.2. Geometry-aware Intra-Patch Representation

While dealing with patches with varying scales, a critical task is to design a feature extractor that generates a fixed-length representation for each patch. To address such an issue, we develop a unified Shared Local Feature Extractor (SLFE) to extract the fixed-length geometry-aware features for all scales of patches.

#### 3.2.1 The *SLFE* Model

Before describing the *SLFE* module, we briefly review the PointNet [23]. Formally, given a disordered point patch  $X^\eta = \{x_1, x_2, \dots, x_{K^\eta}\} \in R^{K^\eta \times C_{in}}$ , PointNet regards  $f : X^\eta \mapsto R$  as a function embedding point set to vector,

$$f(\{x_1, x_2, \dots, x_n\}) = \gamma(\max_{i=1, \dots, K^\eta} \{h(x_i)\}) \quad (2)$$

where  $\gamma$  and  $h$  are usually chosen as MLP networks to map the point cloud features into a high dimensional space for further processing, e.g., from  $N \times 3$  to  $N \times 1024$  in PointNet, where  $N$  denotes the number of points. This mapping function in Eq. (2) could be interpreted as a point’s linear spatial encoder [24], while ignoring the nonlinear geometric structure of the point clouds.

Inspired by the PointNet and its variants, we develop the *SLFE* module, shown in Figure 3, which can be concluded from two aspects: (1) We propose a novel local geometry extractor, sphere mapping, to extract the geometry-aware structures of patches. (2) A pipeline called *SLFE* is proposed. Besides the sphere mapping, the  $h$  used in this work contains the MLP as Eq. 2 of the PointNet and the MRC (MaxPooling, Repeat, Concat) module. Intuitively, as shown in Figure 3, a feature aggregation of  $S^\eta$  patches in the mid-term, i.e., the MaxPooling of the  $K^\eta$  neighbors of each point from a patch, makes the features of a patch more prominent and its semantic information easier to be captured.

**Sphere Mapping** Since the point cloud has strong non-Euclidean geometric properties, its geometric features are challenging to capture correctly in Euclidean space. In the *SLFE* module, we propose a novel sphere mapping, as shown in Figure 3, to map the point cloud features to a sphere space for a better geometric analysis. Formally, we use  $\{P_{i,j}^\eta\}_{j=1, \dots, K^\eta} \in R^{K^\eta \times d}$  to represent the  $K^\eta$  neighbor point of the  $P_i^\eta \in R^d$ , and each neighbor point  $P_{i,j}^\eta$  is the vector with  $d = 64$ . We then use the following formula to transform neighbor points to a sphere:

$$\bar{P}_i^\eta = \frac{1}{K^\eta} \sum_{j=1}^{K^\eta} P_{i,j}^\eta \quad (3)$$

$$\{P_{i,j}^\eta\} = \alpha^\eta \odot \frac{P_{i,j}^\eta - \bar{P}_i^\eta}{|P_{i,j}^\eta - \bar{P}_i^\eta| + \epsilon} \quad (4)$$

$$+ \frac{\beta^\eta}{K^\eta} \odot \sum_{s=1}^{K^\eta} \frac{(P_{i,j}^\eta - \bar{P}_i^\eta)(P_{s,j}^\eta - \bar{P}_i^\eta)}{|P_{i,j}^\eta - \bar{P}_i^\eta| \cdot |P_{s,j}^\eta - \bar{P}_i^\eta| + \epsilon} + b^\eta \quad (5)$$

where  $\alpha^\eta, \beta^\eta, b^\eta \in R^d$  are learnable parameters,  $\odot$  is Hadamard product, and  $\epsilon = 1e^{-5}$  is a stability coefficient

to prevent the denominator to be 0. In Eq. (5), the first term is in charge of mapping the points to a uniform sphere, the second term computes the angles between the  $i^{th}$  point and its neighbors, and the third term  $b^\eta$  is the bias.

Through the sphere mapping module, the local geometric structure of the neighbors of a patch is mapped to a sphere. Hence we can extract the geometric relations (angles) between points in a more efficient way. Therefore, the geometric characteristics of a patch are effectively extracted.

### 3.3. Geometry-aware Inter-Patch Representation

With multi-scale patches and their features at hand, we employ a manifold-based geodesic Transformer to extract the non-Euclidean relations from inter-patches.

#### 3.3.1 From Patch Encoding to Embedding

Obtaining the multi-scale geometric patch representations  $P^\eta \in R^{S^\eta \times K^\eta \times C_{in}}$ , an embedding function  $E_{P^\eta} = SLFE^\eta(P^\eta)$  is performed and then we concatenate the multi-scale embedded patches  $E_p = Concat(E_{P^{sm}}, E_{P^{lg}}) \in R^{S \times d_{out}}$  for geodesic self-attention computation.

#### 3.3.2 Class Tag and Position Encoding

Before the self-attention computation, we concatenate the class tag and implement the position encoding to the embedded features for better convergence. Similar to the claims in BERT[4] and ViT[6], we randomly initialize a learning-available class token  $E_0 \in R^{d_{out}}$ , and then stitch it with point cloud embedding  $E_p$  to get the total sequence  $E \in R^{(S+1) \times d_{out}}$ .

In the original Transformer, a position encoding module is applied to represent the order in natural language, which can reflect the position relationship between words. In this paper, in order to reflect the position relationship between the point cloud patches, we also add position encoding to the point cloud embedded to retain the location information. Considering that the point cloud data itself has location information, we use the center point coordinates of each point cloud patch to represent the location information of each point cloud patch. Specifically, we randomly initialize the class tag to  $CT_{cls} \in R^3$  and then stitch with the central point coordinate of each point cloud patch, and then use a learned MLP layer to map the central point coordinate to the embedded dimension ( $d_{out}$ ), then get the position encoding  $E_{pos} \in R^{(S+1) \times d_{out}}$ .

#### 3.3.3 Transformer Encoder

Following the pipeline of Transformer, the modified Transformer encoder is applied for feature encoding. The Trans-

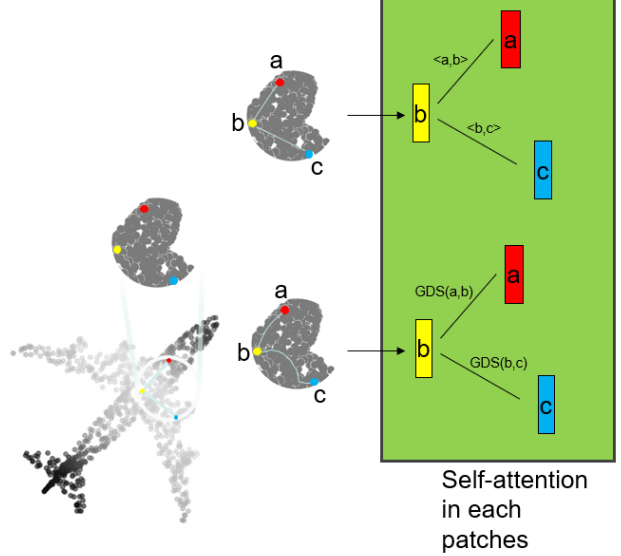


Figure 4. Comparison between dot product-based self-attention and geodesic-distance-based self-attention on point cloud. Top: dot product-based self-attention. Bottom: geodesic-distance-based self-attention.

former encoder includes *MGT* with adjustable levels of patches. To extract the non-Euclidean inter-patch relationship, we implement the manifold-based geodesic self-attention to modify the self-attention module. We assume that for the point cloud, a typical non-Euclidean data, we should utilize the geodesic distance between its feature points rather than the inner product in Euclidean space to capture its relative relationship. For the input sequence  $z$ , we project the original features in Euclidean space onto an oblique manifold [1], i.e., a unit length Spheres denoted by  $\mathcal{OM}$ , and compute the geodesic self-attention of the patch features embedded on the oblique manifold. All concepts on geodesic and manifold are referred to [1, 10]. The projection function  $Proj(\cdot)$  can be described as:

$$P := Proj(z) = Cat \left( \left\{ \frac{z_i}{\|z_i\|} \right\}_{i=0}^L \right), \quad (6)$$

where  $Cat(\cdot)$  denotes concatenate function and  $\|\cdot\|$  denotes the square Frobenius norm in the ambient space.

After the projection, the geodesic distance of an input pair of points  $\{Q, K\}$  on  $\mathcal{OM}$  can be calculated as:

$$dist(Q, K) = \sqrt{\sum_{i=1}^n \arccos^2 \left( \text{diag} \left( Q^T K \right) \right)_i}, \quad (7)$$

Therefore, the output of the *MGT* module  $z_{out}$  can be calculated as:

$$z_{out} = softmax(-GDS(z)) \cdot W_v(z), \quad (8)$$

Equipment	Name
Operation System	Linux
GPU	NVIDIA GEFORCE RTX 2080Ti(8)
Framework	Pytorch1.8.1+cu101
Language	Python3.7

Table 1. Experimental environment and configuration. Each group of experiments only uses one GPU, and eight are only comparative tests of multiple groups.

where  $GDS(\cdot)$  is the geodesic distance computation function defined in Eq. (7) and  $W_v$  is a linear layer.

Then, we input the sequence  $z_0$  with the position encoding obtained in Section 3.3.1 into the aforementioned Transformer Encoder with  $L$  layers (LN means LayerNorm). The specific process is as follows:

$$z_l = MGT(LN(z_{l-1})) + z_{l-1}, l = 1, \dots, L \quad (9)$$

$$z_l = MLP(LN(z_l)) + z_l, l = 1, \dots, L$$

$$y = LN(z_L^0), y \in R^{d_{out}} \quad (10)$$

After above steps, the class token  $y$  with global classification information is obtained in the first element of the output sequence.

## 4. Experiments

In this section, we evaluate the multi-class classification performance of our proposed *MGT* framework on several benchmarks.

In the ablation studies, we perform both qualitative and quantitative assessments of the *MGT* framework’s effectiveness. Some additional experiments are illustrated in supplementary materials.

### 4.1. Experimental Environment and Configuration

In training, we use the label smooth cross-entropy loss function [21]. The batch size and the number of the epoch are set as 32 and 250, respectively.

The SGD optimizer and CosineAnnealingLR are used to adjust the learning rate, and the initial learning rate is 0.02. The configuration of the machine is shown in Table 1.

Moreover, the overall accuracy (OA) and class-wise mean accuracy (mAcc) are used as the performance evaluation criteria for classification.

Unless explicitly stated in the experimental study, we input 1024 (1K) points and do not adopt the normal vector as the original point feature.

### 4.2. 3D Object Classification

The *Modelnet40* [38] dataset contains 40 categories of 12311 grid CAD models, including 9843 training models and 2468 test models. For each data model, the sample of

Method	Input	#Points	OA%	mAcc%
Pointnet[23]	$xyz$	1K	89.2	86.2
PointNet++[24]	$xyz$	1K	90.7	-
	$xyz + n$	5K	91.9	-
PointWeb[46]	$xyz$	1K	92.3	89.4
SO-Net[16]	$xyz + n$	2K	90.9	87.3
	$xyz + n$	5K	93.1	<b>90.9</b>
PointConv[37]	$xyz$	1K	92.5	-
DGCNN[36]	$xyz$	1K	92.9	90.5
PCT[8]	$xyz$	1K	93.1	-
MLMSPT[9]	$xyz$	1K	<u>92.9</u>	-
Ours	$xyz$	1K	92.14	90.38
Ours	$xyz + n$	1K	<b>93.19</b>	<u>90.45</u>

Table 2. Classification performance of mainstream methods on *ModelNet40* dataset. The optimal results in the table are shown in **bold**, and the sub-optimal results are shown in underline.

the grid surface  $N = 1024$  points with normalized coordinates being the input of the network. During the training process, in order to improve the diversity of the sample, the following operations are adopted to enrich the data: 1) Randomly zoomed in the internal scale  $[-0.8, 1.25]$ ; 2) Gaussian noise with the mean of 0 and the variance of 0.02 to shift each point Location; 3) Randomly discard some points with not exceeding 12.5% of the total number of points.

*ScanObjectNN* [31] dataset is a real-world dataset. The sample contains not only the target itself, but also background information and noise interference. Therefore, this dataset is more real, complex, and challenging. *ScanObjectNN* contains 15,000 objects, divided into 15 and 2902 unique object instances. In training, we use the same data augmentation methods as *Modelnet40*.

To verify the effectiveness of the proposed method, we will compare it with some mainstream methods. The results on *ModelNet40* and *ScanObjectNN* datasets are shown in Table 2 and Table 3, respectively ( $xyz$  is the coordinate,  $n$  is the normal vector).

The experimental results of Table 2 and Table 3 show that the proposed method has demonstrated very competitive results when compared with some mainstream methods. On the *Modelnet40* dataset, the algorithms of this paper achieved 93.19% and 90.45% on the OA and mAcc indicators, respectively. The strongly competitive results on the two benchmark datasets show the effectiveness of the proposed method in comparison with the aforementioned baselines.

### 4.3. Ablation Experiments

In this paper, we use the SLFE to encode the point cloud into point cloud embedding. In the experiment, it is found that using the original PointNet++ as the local feature extractor is difficult to achieve ideal results. To this end, we

	3DmFV [2]	Pointnet	Pointnet++	SpiderCNN [41]	DGCNN	PointCNN [17]	PointConv	Ours
mAcc	58.3	63.9	75.4	69.8	73.6	75.1	74.1	<b>78.59</b>
OA	63.9	68.2	78.9	73.7	78.1	78.5	77.4	<b>80.47</b>

Table 3. Classification performance of mainstream methods on ScanObjectNN dataset. The optimal results in the table are shown in **bold**

local feature extractor	Parameters	OA%	mAcc%
PointNet	1.87M	90.80	87.92
SLFE(Single)	0.31M	93.31	90.63

Table 4. Comparison Experiment of feature extractor using PointNet and SLFE on ModelNet40

No.	Sphere Mapping	MRC	OA%	mAcc%
<i>A</i>	×	×	90.54	87.64
<i>B</i>	×	✓	91.73	88.34
<i>C</i>	✓	×	92.31	90.37
<i>D</i>	✓	✓	93.31	90.63

Table 5. Ablation experiments on *ModelNet40*. × indicates the experiment without the corresponding module, and ✓ indicates the experiment with the corresponding module

draw on the ideas of PointNet, and develop a lightweight SLFE as a local feature extractor, which can have a better performance.

In this section, we compare the experimental results by using the original PointNet and SLFE.

The experimental results in Table 4 show that a single SLFE has only 0.31M parameters, but the results by using SLFE are 2.51% and 2.71% higher than those using PointNet on OA and mAcc, respectively.

This indicates that the developed SLFE is effective as a local feature extractor. The ablation experiment, test results on ModelNet40 dataset, in Table 5 discusses the necessity of SLFE in the modules.

According to the analysis of the ablation experiment results in the table, *A* had the worst result without adding Sphere Mapping module and maximum pooling module. Intuitively, in the middle term, feature aggregation is conducted for each point cloud. That is, the point features of each patch are pooled to the maximum, and the obtained local features are spliced with the features before aggregation to highlight the local features and make the local semantic information more distinct. The OA result in *B* is 1.19% higher than that in *A*, which indicates that this operation is effective and confirms our assumption. The OA result in *C* is 1.77% higher than that in *A*, and the Sphere Mapping module maps the local features to the unit length sphere, thus implicitly encoding the local geometric information and angles, making up for the lack of geometric information. So that all point clouds of the same size can better extract the local geometric features when sharing a local

	<i>ModelNet40</i>		<i>ScanObjectNN</i>	
	OA%	mAcc%	OA%	mAcc%
Dot product	92.1	89.38	79.47	76.57
Geodesic-distance	92.21	89.96	79.99	76.82

Table 6. Experimental results on different self-attention methods

Number of scales	<i>ScanObjectNN</i>	
	OA%	mAcc%
1	79.68	77.20
2	79.85	77.52
3	79.99	77.77

Table 7. Experimental results in different numbers of scales

feature encoder. It is similar to the operation in *B*, that is, it highlights the local information and makes the local semantic information more distinct, which lays a good foundation for the later Transformer Encoder module to capture the relationship between local features. The results in *D* show that *B* and *C* operations complement each other and make the algorithm obtain the optimal results.

Also, in this section, we have discussed at length the impact of the geodesic-distance-based self-attention mechanism on the experimental results. In Table 6, we compared the experimental results of the traditional self-attention mechanism using dot product with the self-attention mechanism based on geodesic distance. The experimental results in the table show that the use of the geodesic distance-based self-attention mechanism improved the results on both the ModelNet40 and ScanobjectNN datasets. On the ModelNet40 dataset, using the geodesic-distance-based self-attention mechanism improved OA by 0.11% and mAcc by 0.58% compared to using the traditional dot product-based self-attention mechanism. For the ScanobjectNN dataset, OA was improved by 0.52% and mAcc was improved by 0.25%. This result indicates that for point cloud data, using the geodesic distance on the manifold surface to express weights is more suitable than the traditional dot product.

In addition, we also explored the impact of the number of scales on classification accuracy. Table 7 shows the different effects on experimental results by dividing point cloud data into different scales in Multi-scale Division. The ScanobjectNN dataset was used in the experiment. The results demonstrate that the multi-scale transformer performs better than the single-scale transformer. Dividing point cloud data into more scales allows more diverse data

Point Numbers	OA%	mAcc%
512	78.99	76.08
1024	79.47	76.57
2048	79.71	77.27

Table 8. The effect of the number of points in a point cloud on the experimental results.

	<i>ModelNet40</i>		<i>ScanObjectNN</i>	
	OA%	mAcc%	OA%	mAcc%
Direct training	93.31	90.63	82.81	81.91
Transfer Learning	94.03	91.28	83.52	82.77

Table 9. Model performances with Transfer learning

to enter the transformer, thus providing more point cloud structural information. The scale with more points but fewer patches provides more detailed global feature about the point cloud, while the scale with fewer points but more patches provides more detailed local feature .

#### 4.4. Point Number and Patch size

In this section, we will discuss the experimental results of point cloud data with different point numbers. The experiment is based on the classification task on ScanobjectNN dataset.

We conducted experiments on point cloud data with different numbers of points within the same dataset in Table 8. Each experiment used a different number of points extracted from the dataset for calculation. We conducted experiments on the ScanobjectNN dataset with 512 points, 1024 points, and 2048 points, respectively. As shown in the table, the accuracy of *MGT* gradually increased as the number of points in the dataset increased.

#### 4.5. Transfer Learning

The research of ViT point out that when the amount of training data is large enough, the global context modeling based on Transformer has stronger expression ability. Therefore, this paper conducts a migration learning experiment from a larger dataset to a smaller dataset.

ShapeNetCore v2 contains 55 categories of 51300 3D models in total. We divide the entire data set into a training set and a verification set, but only perform pre-training on the training set. For each instance model, we use the FPS algorithm to uniformly sample 1024 points as the point cloud input data. Note that, unlike the data enhancement in ModelNet40 and ScanObjectNN, we apply standard random scaling and random translation to enhance the data. During pre-training, Adam optimizer and CosineAnnexingLR are used to adjust the learning rate. The initial learning rate is set to 0.03, weight\_decay is 0.005, batchsize is 64, and the epoch is 250.

Compared with direct training, it can be seen from Table 9 that when a large dataset, ShapeNetCore v2, is used for pre-training first, and then fine-tuning on the ModelNet40 dataset, the accuracy of OA and mAcc of this method are 94.03% and 91.28%, respectively. Fine-tuning in the ScanObjectNN dataset achieved 83.52% and 82.77% in accuracy, respectively. Therefore, the proposed method in this paper effectively inherits the excellent migration capability of Transformer architecture.

#### 4.6. Robustness Test and Analysis

The experiments above verified that the proposed method is simple and effective in classification. This section will test the robustness of the model on data point loss. The index in this section is the OA of the model training conducted on the ModelNet40 training set (1K points), and then testing on the test set (the farthest point sampled with missing data).

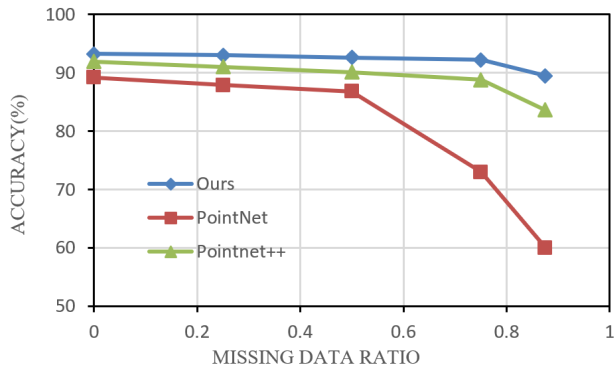


Figure 5. Model performances with missing points.

In this paper, PointNet and Pointnet++, are selected as the comparative to test the robustness with point cloud loss (data with missing points). As shown in Figure 5, when the farthest point sampling is used to make the point cloud data of the test set lose 50% (i.e. 512 points are retained), the accuracy rate only decreases by 0.6%, which is lower than 1.8% and 2.4% of the decline of Pointnet++ and Pointnet. When the ratio of lost points is 87.5% (that is, 128 points are retained), the algorithm in this paper can still achieve an excellent accuracy of 89.5%, and Pointnet++ is 83.6%, while PointNet can only achieve an accuracy of 60%, with a significant decline in accuracy. This indicates that the proposed method has strong robustness on point cloud data with missing points. The experiment shows that, when the recognition model can use the local information of the point cloud, it can be more robust to the loss of point cloud data (missing points). The proposed method can still have a high accuracy facing a high loss rate of point cloud data, owing to the full use of the rich local semantic information of point cloud and the excellent global modeling ability of Trans-

former Encoder architecture to capture the relationship between local semantic information.

## 5. Conclusion

In order to explore the complex geometric structures hidden in point clouds, this paper proposed a novel Transformer framework, *MGT*, for the classification of point cloud objects. At first, we divide the data into multi-scale patches with different sizes, i.e., from small size to large size of patches, to explore the multiple scales of structures of point clouds. Then, we construct a geometry-aware transformer model, which leverages two-level geometric structures, i.e., the Euclidean geometry of each intra-patch and the non-Euclidean geometry of inter-patches of point clouds. The former is achieved by a local sharing feature extractor associated with a novel sphere mapping module, while the latter is accomplished using a manifold-based self-attention module. Compared with the mainstream methods, the accuracy of the proposed method on point cloud recognition has shown strong competitiveness and good robustness in the face of data point loss. In future, the proposed method can be extended to more point cloud processing tasks, such as object detection and scene segmentation.

## References

- [1] P-A Absil, Robert Mahony, and Rodolphe Sepulchre. *Optimization algorithms on matrix manifolds*. Princeton University Press, 2008.
- [2] Yizhak Ben-Shabat, Michael Lindenbaum, and Anath Fischer. 3dmfv: Three-dimensional point cloud classification in real-time using convolutional neural networks. *IEEE Robotics and Automation Letters*, 3(4):3145–3152, 2018.
- [3] Xiaozhi Chen, Huimin Ma, Ji Wan, Bo Li, and Tian Xia. Multi-view 3d object detection network for autonomous driving. In *Proceedings of the IEEE conference on Computer Vision and Pattern Recognition*, pages 1907–1915, 2017.
- [4] Jacob Devlin, Ming-Wei Chang, Kenton Lee, and Kristina Toutanova. Bert: Pre-training of deep bidirectional transformers for language understanding. *arXiv preprint arXiv:1810.04805*, 2018.
- [5] Ming Ding, Wendi Zheng, Wenyi Hong, and Jie Tang. Cogview2: Faster and better text-to-image generation via hierarchical transformers. *arXiv preprint arXiv:2204.14217*, 2022.
- [6] Alexey Dosovitskiy, Lucas Beyer, Alexander Kolesnikov, Dirk Weissenborn, Xiaohua Zhai, Thomas Unterthiner, Mostafa Dehghani, Matthias Minderer, Georg Heigold, Sylvain Gelly, et al. An image is worth 16x16 words: Transformers for image recognition at scale. *arXiv preprint arXiv:2010.11929*, 2020.
- [7] Yanhong Fei, Ming Hu, Xian Wei, and Mingsong Chen. Orthogonal spatial-temporal graph convolutional networks for traffic flow forecasting. In *2022 IEEE Symposium Series on Computational Intelligence (SSCI)*, pages 71–76, 2022.
- [8] Meng-Hao Guo, Jun-Xiong Cai, Zheng-Ning Liu, Tai-Jiang Mu, Ralph R Martin, and Shi-Min Hu. Pct: Point cloud transformer. *Computational Visual Media*, 7(2):187–199, 2021.
- [9] Xian-Feng Han, Yu-Jia Kuang, and Guo-Qiang Xiao. Point cloud learning with transformer. *arXiv preprint arXiv:2104.13636*, 2021.
- [10] Simon Hawe, Matthias Seibert, and Martin Kleinsteuber. Separable dictionary learning. In *Proceedings of the IEEE Conference on Computer Vision and Pattern Recognition (CVPR)*, pages 438–445. IEEE, June 2013.
- [11] Kaiming He, Xinlei Chen, Saining Xie, Yanghao Li, Piotr Dollár, and Ross Girshick. Masked autoencoders are scalable vision learners. In *Proceedings of the IEEE/CVF Conference on Computer Vision and Pattern Recognition*, pages 16000–16009, 2022.
- [12] Lun Huang, Wenmin Wang, Jie Chen, and Xiaoyong Wei. Attention on attention for image captioning. In *ICCV*, pages 4633–4642, 2019.
- [13] Asako Kanezaki, Yasuyuki Matsushita, and Yoshifumi Nishida. Rotationnet: Joint object categorization and pose estimation using multiviews from unsupervised viewpoints. In *Proceedings of the IEEE conference on computer vision and pattern recognition*, pages 5010–5019, 2018.
- [14] Hai Lan, Xihao Wang, Hao Shen, Peidong Liang, and Xian Wei. Couplformer: Rethinking vision transformer with coupling attention. In *2023 IEEE/CVF Winter Conference on Applications of Computer Vision (WACV)*, pages 6464–6473, 2023.
- [15] JDMCK Lee and K Toutanova. Pre-training of deep bidirectional transformers for language understanding. *arXiv preprint arXiv:1810.04805*, 2018.
- [16] Jiaxin Li, Ben M Chen, and Gim Hee Lee. So-net: Self-organizing network for point cloud analysis. In *Proceedings of the IEEE conference on computer vision and pattern recognition*, pages 9397–9406, 2018.
- [17] Yangyan Li, Rui Bu, Mingchao Sun, Wei Wu, Xinhan Di, and Baoquan Chen. Pointcnn: Convolution on x-transformed points. *Advances in neural information processing systems*, 31, 2018.
- [18] Zhengyu Li, Xuan Tang, Zihao Xu, Xihao Wang, Hui Yu, Mingsong Chen, and Xian Wei. Geodesic self-attention for 3d point clouds. In *Advances in Neural Information Processing Systems*.
- [19] Xinhai Liu, Zhizhong Han, Yu-Shen Liu, and Matthias Zwicker. Point2sequence: Learning the shape representation of 3d point clouds with an attention-based sequence to sequence network. In *Proceedings of the AAAI conference on artificial intelligence*, volume 33, pages 8778–8785, 2019.
- [20] Daniel Maturana and Sebastian Scherer. Voxnet: A 3d convolutional neural network for real-time object recognition. In *2015 IEEE/RSJ international conference on intelligent robots and systems (IROS)*, pages 922–928. IEEE, 2015.
- [21] Rafael Müller, Simon Kornblith, and Geoffrey E Hinton. When does label smoothing help? *Advances in neural information processing systems*, 32, 2019.
- [22] Yatian Pang, Wenxiao Wang, Francis EH Tay, Wei Liu, Yonghong Tian, and Li Yuan. Masked autoencoders for point cloud self-supervised learning. In *Computer Vision—ECCV 2022: 17th European Conference, Tel Aviv, Israel, October 23–27, 2022, Proceedings, Part II*, pages 604–621. Springer, 2022.
- [23] Charles R Qi, Hao Su, Kaichun Mo, and Leonidas J Guibas. Pointnet: Deep learning on point sets for 3d classification and segmentation. In *Proceedings of the IEEE conference on computer vision and pattern recognition*, pages 652–660, 2017.
- [24] Charles Ruizhongtai Qi, Li Yi, Hao Su, and Leonidas J Guibas. Pointnet++: Deep hierarchical feature learning on point sets in a metric space. *Advances in neural information processing systems*, 30, 2017.
- [25] Prajit Ramachandran, Niki Parmar, Ashish Vaswani, Irwan Bello, Anselm Levskaya, and Jon Shlens. Stand-alone self-attention in vision models. *Advances in Neural Information Processing Systems*, 32, 2019.
- [26] Aurko Roy, Mohammad Saffar, Ashish Vaswani, and David Grangier. Efficient content-based sparse attention with routing transformers. *Trans. Assoc. Comput. Linguistics*, 9:53–68, 2021.
- [27] Radu Bogdan Rusu, Zoltan Csaba Marton, Nico Blodow, Mihai Dolha, and Michael Beetz. Towards 3d point cloud based object maps for household environments. *Robotics and Autonomous Systems*, 56(11):927–941, 2008.

- [28] Shaoshuai Shi, Chaoxu Guo, Li Jiang, Zhe Wang, Jianping Shi, Xiaogang Wang, and Hongsheng Li. Pv-rcnn: Point-voxel feature set abstraction for 3d object detection. In *Proceedings of the IEEE/CVF Conference on Computer Vision and Pattern Recognition*, pages 10529–10538, 2020.
- [29] Shaoshuai Shi, Xiaogang Wang, and Hongsheng Li. Pointcnn: 3d object proposal generation and detection from point cloud. In *Proceedings of the IEEE/CVF conference on computer vision and pattern recognition*, pages 770–779, 2019.
- [30] Hugues Thomas, Charles R Qi, Jean-Emmanuel Deschaud, Beatriz Marcotegui, François Goulette, and Leonidas J Guibas. Kpconv: Flexible and deformable convolution for point clouds. In *Proceedings of the IEEE/CVF international conference on computer vision*, pages 6411–6420, 2019.
- [31] Mikaela Angelina Uy, Quang-Hieu Pham, Binh-Son Hua, Thanh Nguyen, and Sai-Kit Yeung. Revisiting point cloud classification: A new benchmark dataset and classification model on real-world data. In *Proceedings of the IEEE/CVF international conference on computer vision*, pages 1588–1597, 2019.
- [32] Ashish Vaswani, Noam Shazeer, Niki Parmar, Jakob Uszkoreit, Llion Jones, Aidan N Gomez, Łukasz Kaiser, and Illia Polosukhin. Attention is all you need. *Advances in neural information processing systems*, 30, 2017.
- [33] Fei Wang, Mengqing Jiang, Chen Qian, Shuo Yang, Cheng Li, Honggang Zhang, Xiaogang Wang, and Xiaoou Tang. Residual attention network for image classification. In *Proceedings of the IEEE conference on computer vision and pattern recognition*, pages 3156–3164, 2017.
- [34] Xihao Wang, Jiaming Lei, Hai Lan, Arafat Al-Jawari, and Xian Wei. Dueqnet: Dual-equivariance network in outdoor 3d object detection for autonomous driving, 2023.
- [35] Xihao Wang and Xian Wei. Continual learning for pose-agnostic object recognition in 3d point clouds. *arXiv preprint arXiv:2209.04840*, 2022.
- [36] Yue Wang, Yongbin Sun, Ziwei Liu, Sanjay E Sarma, Michael M Bronstein, and Justin M Solomon. Dynamic graph cnn for learning on point clouds. *Acm Transactions On Graphics (tog)*, 38(5):1–12, 2019.
- [37] Wenxuan Wu, Zhongang Qi, and Li Fuxin. Pointconv: Deep convolutional networks on 3d point clouds. In *Proceedings of the IEEE/CVF Conference on Computer Vision and Pattern Recognition*, pages 9621–9630, 2019.
- [38] Zhirong Wu, Shuran Song, Aditya Khosla, Fisher Yu, Linguang Zhang, Xiaoou Tang, and Jianxiong Xiao. 3d shapenets: A deep representation for volumetric shapes. In *Proceedings of the IEEE conference on computer vision and pattern recognition*, pages 1912–1920, 2015.
- [39] Saining Xie, Sainan Liu, Zeyu Chen, and Zhuowen Tu. Attentional shapecontextnet for point cloud recognition. In *Proceedings of the IEEE conference on computer vision and pattern recognition*, pages 4606–4615, 2018.
- [40] Haiyang Xu, Ming Yan, Chenliang Li, Bin Bi, Songfang Huang, Wenming Xiao, and Fei Huang. E2e-vgp: end-to-end vision-language pre-training enhanced by visual learning. *arXiv preprint arXiv:2106.01804*, 2021.
- [41] Yifan Xu, Tianqi Fan, Mingye Xu, Long Zeng, and Yu Qiao. Spidercnn: Deep learning on point sets with parameterized convolutional filters. In *Proceedings of the European Conference on Computer Vision (ECCV)*, pages 87–102, 2018.
- [42] Haoxuan You, Yifan Feng, Rongrong Ji, and Yue Gao. Pvnnet: A joint convolutional network of point cloud and multi-view for 3d shape recognition. In *Proceedings of the 26th ACM international conference on Multimedia*, pages 1310–1318, 2018.
- [43] Xumin Yu, Lulu Tang, Yongming Rao, Tiejun Huang, Jie Zhou, and Jiwen Lu. Point-bert: Pre-training 3d point cloud transformers with masked point modeling. In *Proceedings of the IEEE/CVF Conference on Computer Vision and Pattern Recognition*, pages 19313–19322, 2022.
- [44] Manzil Zaheer, Satwik Kottur, Siamak Ravanbakhsh, Barnabas Poczos, Russ R Salakhutdinov, and Alexander J Smola. Deep sets. *Advances in neural information processing systems*, 30, 2017.
- [45] Hengshuang Zhao, Jiaya Jia, and Vladlen Koltun. Exploring self-attention for image recognition. In *Proceedings of the IEEE/CVF Conference on Computer Vision and Pattern Recognition*, pages 10076–10085, 2020.
- [46] Hengshuang Zhao, Li Jiang, Chi-Wing Fu, and Jiaya Jia. Pointweb: Enhancing local neighborhood features for point cloud processing. In *Proceedings of the IEEE/CVF conference on computer vision and pattern recognition*, pages 5565–5573, 2019.
- [47] Hengshuang Zhao, Li Jiang, Jiaya Jia, Philip HS Torr, and Vladlen Koltun. Point transformer. In *Proceedings of the IEEE/CVF International Conference on Computer Vision*, pages 16259–16268, 2021.
- [48] Yin Zhou and Oncel Tuzel. Voxelnet: End-to-end learning for point cloud based 3d object detection. In *Proceedings of the IEEE conference on computer vision and pattern recognition*, pages 4490–4499, 2018.
- [49] Xizhou Zhu, Weijie Su, Lewei Lu, Bin Li, Xiaogang Wang, and Jifeng Dai. Deformable DETR: deformable transformers for end-to-end object detection. In *ICLR*, 2021.